Electrical Conductivity of Decamethylferrocenium Hexafluorophosphate and Tetrabutylammonium Hexafluorophosphate in Supercritical Trifluoromethane

Darío L. Goldfarb[†,‡] and Horacio R. Corti*[,†,§]

Comisión Nacional de Energía Atómica, Unidad de Actividad Química, Av. Gral. Paz 1499 (1650) San Martín, Buenos Aires, Argentina, and Departamento de Química Inorgánica, Analítica y Química Física, Facultad de Ciencias Exactas y Naturales, Universidad de Buenos Aires, Pabellón II, Ciudad Universitaria (1428), Buenos Aires, Argentina

Received: February 27, 2003; In Final Form: November 29, 2003

The electrical conductivity of tetrabutylammonium hexafluorophosphate ($TBAPF_6$) and decamethylferrocenium hexafluorophosphate ($Fe(Cp^*)_2PF_6$) in supercritical trifluoromethane (CHF_3) was measured as a function of density (at pressures of 6−16 MPa) at 323.15 K. The concentration dependence of the molar conductivity was fitted using the Fuoss−Kraus equations, including ion pairs and triplets, and the molar conductivities at infinite dilution and the ion-pair formation constants were calculated as a function of the solvent density for both salts. The results were analyzed and explained by resorting to the peculiar properties of supercritical fluids in the low-density region. A comparison with the continuum model of ion mobility was conducted to demonstrate the inability of such a hydrodynamic model to describe the transport properties of salts in supercritical media. Also, the compressible continuum model applied to these systems seems to describe the limiting conductivity behavior in the high-density region rather well.

Introduction

Interest in the study of transport processes in supercritical solvents has increased recently, because of the fact that the high mass-transfer coefficients observed in these highly compressible fluids make them potential solvents for industrial applications. From a basic point of view, the main features of transport processes in supercritical solvents are not well understood yet; it is a field that is full of tremendous theoretical and experimental challenges.

It is not unexpected that the pioneering work in supercritical fluids was conducted in aqueous solutions. Studies of the electrical conductances of simple electrolytes in supercritical water performed by Fogo et al.,[1] Franck,[2] and Quist and Marshall[3] during the 1950s were restricted to densities of >0.3 g/cm^3 and salt concentrations of >0.001 mol dm^{-3}.

More recently, Ho and co-workers[4−6] modified the cell that was used by Marshall, extending the range of temperatures and densities and improving the precision of the data for several electrolytes. Wood and co-workers[7,8] developed a flow cell to measure electrical conductances of very dilute electrolytes (down to 4×10^{-8} mol dm^{-3}) in supercritical water at temperatures up to 674 K and densities of 0.2−0.7 g/cm^3. Also, Bard and co-workers[9,10] measured the diffusion coefficients of several solutes in supercritical water at different densities, using cyclic voltammetry (CV), chronoamperometry, and chronocoulometry. They also studied the diffusion of solutes in other supercritical fluids that have a high dielectric constant, such as NH_3,[11,12] SO_2,[13] and CH_3CN.[14,15]

However, the fact that water and other polar solvents have very high critical pressures and temperatures makes accurate determination of the transport coefficients in the supercritical region very difficult and discourages their use on industrial scales.

Carbon dioxide (CO_2), which is the preferred supercritical solvent for industrial applications, because of its low critical parameters and low cost and toxicity, is a poor solvent for ionic solutes. Wightman et al.[16] and Abbott and Harper[17] performed CV studies in supercritical CO_2 using tetrahexylammonium hexafluorophosphate ($THAPF_6$) and tetradecylammonium tetraphenylborate ($TDABPh_4$) as the supporting electrolyte; however, they were unsuccessful in their attempts to obtain precise limiting currents for diffusion measurements, because of the incipient ohmic distortion of the voltammograms.

Olsen and Tallman[18,19] were the first to use hydrofluorocarbons (HFCs) for electrochemical experiments in supercritical solvents. They measured the diffusion coefficients of ferrocene and cobaltocenium hexafluorophosphate in chlorodifluoromethane (critical dielectric constant of $\epsilon_c = 2.31$, critical temperature of $T_c = 369.2$ K, and critical pressure of $p_c = 4.97$ MPa), using tetrabutylammonium tetrafluoroborate ($TBABF_4$) as the supporting electrolyte, at densities of 0.81−1.02 g/cm^3.

Abbott et al.[20] also performed electrochemical measurements in supercritical 1,1,1,2-tetrafluoroethane ($\epsilon_c = 3.5$) and difluoromethane ($\epsilon_c = 4.9$), with $TBAClO_4$ as the supporting electrolyte. Although these solvents have higher relative permittivities than $CHClF_2$ at the critical point, their overpotential window is very wide. More recently, Abbott and Eardley[21] measured the electrical conductivity of $TBABF_4$ in subcritical 1,1,1,2-tetrafluoroethane and in difluoromethane in the subcritical and supercritical states, as a function of concentration (c) and pressure (p) and obtained the ion-pair and triple-ion dissociation constants. Their measurements were performed on a relatively concentrated solution ($c > 10^{-3}$ mol dm^{-3}), and, for this reason, the molar conductivity at infinite dilution could

* Author to whom correspondence should be addressed. E-mail: hrcorti@cnea.gov.ar.

† Comisión Nacional de Energía Atómica.

‡ Present address: Advanced Lithography Materials and Processes, IBM Thomas J. Watson Research Center, P.O. Box 218, Yorktown Heights, NY 10598.

§ Universidad de Buenos Aires.

10.1021/jp0345102 CCC: $27.50 © 2004 American Chemical Society
Published on Web 02/17/2004

not be extrapolated from the experimental data; instead, it was estimated by assuming the validity of Walden's rule under the conditions studied.

The appeal of HFCs as supercritical solvents for application in transport studies is their mild critical parameters, the larger potential window for voltammetric studies (as compared to water), and the relatively good solubility of bulky ions. Recently,[22] we have shown that CHF_3 is a suitable fluid to study the transport properties of ions in variable-density solvents that have a low dielectric constant. We have shown that precise voltammetric determinations of the diffusional current can be performed with decamethylferrocene ($Fe(Cp^*)_2$) and decamethylferrocenium hexafluorophosphate ($Fe(Cp^*)_2PF_6$) as electroactive species in supercritical CHF_3, using tetrabutylammonium hexafluorophosphate ($TBAPF_6$) as the supporting electrolyte and microelectrode techniques. We also reported the solubility and electrical conductances of the salts and proposed the system as a model for systematic studies of the transport properties of ionic and neutral solutes in supercritical fluids.

In this work, we performed a comprehensive study of the electrical conductivity of $Fe(Cp^*)_2PF_6$ and $TBAPF_6$ in supercritical CHF_3 at 323.15 K over a wide range of densities, to obtain information on the speciation (as affected by ion association) and limiting conductivities of both electrolytes. The main objective of this study is to analyze the applicability of transport models valid for normal liquids to the supercritical regime. This is also the objective of the accompanying article,[23] where we use a voltammetric technique with microelectrodes to determine the diffusion coefficients of $Fe(Cp^*)_2PF_6$ and $Fe(Cp^*)_2$ in supercritical CHF_3. Both techniques are complementary, because the trace diffusion coefficient of the ionic species (D_i) is related to the ionic limiting molar conductivity (λ_i°) by the well-known Nernst−Einstein relationship. At the same time, the sum of the λ_i° values for the individual ions is equal to the limiting molar conductivity of the salt (Λ°) determined in this study for $Fe(Cp^*)_2PF_6$ and $TBAPF_6$. The electrical conductivity technique also provides an insight to the speciation of the electrolytes in supercritical fluids, which is strongly dependent on its density.

Experimental Section

Trifluoromethane (>99% CHF_3, K. H. Muller Laboratories) was stored in a stainless-steel cylinder that contained KOH, to eliminate traces of water. CHF_3 was recovered after use by distillation at −78 °C (using an acetone−CO_2 mixture) and received in a cylinder that contained KOH, immersed in liquid nitrogen. $TBAPF_6$ (Fluka, electrochemical grade) was used as received. $Fe(Cp^*)_2PF_6$ was synthesized following a procedure described in a previous work.[24] The solid was dried at 110 °C for 12 h and was used without recrystallization. All solids were stored in a vacuum desiccator.

The high-pressure cell used for the conductivity measurements has been described by Fernandez et al.[25] The cell, which was originally designed for dielectric constant determinations, has two concentric stainless-steel cylinders, and it was calibrated by measuring its capacitance under vacuum. The very low constant of the cell ($\Lambda^\circ = 0.27457\ m^{-1}$ at 323.15 K) makes it suitable for very precise electrical conductivity measurements in highly resistive media, such as supercritical fluids with a low dielectric constant.

The experimental setup for these measurements has been described elsewhere.[22] Briefly, the solute dissolved in dichloromethane is charged into the cell by means of a preweighted syringe. The dichloromethane is evaporated under vacuum and the cell is thermostatized by immersion in a water bath whose temperature was controlled at 323.15 K (within 0.02 K). CHF_3 from the storage cylinder is loaded into a high-pressure manual pump and then transferred to the conductivity cell through a valve until the pressure reaches the selected value. Pressure in the system was measured with a pressure transducer (Burster, $p = 0-20$ MPa) thermostatized at 303.15 K. The transducer was previously calibrated with a dead-weight balance (Ruska) that had an accuracy of 0.005 MPa.

A component analyzer (Wayne Kerr, model 6425) was used to measure the resistance of the fluids under study. A 0.1-V sinusoidal signal was applied to the cell electrodes in the frequency range between 500 Hz and 10 kHz.

TABLE 1: Properties of CHF_3 at Several Densities (T = 323.15 K)

density, ρ (g/cm^3)	dielectric constant, ϵ	viscosity, η (mPa s)	density, ρ (g/cm^3)	dielectric constant, ϵ	viscosity, η (mPa s)
0.900	5.66	0.06803	0.600	3.57	0.03893
0.850	5.27	0.06197	0.550	3.28	0.03556
0.800	4.90	0.05644	0.500	3.00	0.03247
0.750	4.54	0.05141	0.400	2.49	0.02718
0.700	4.20	0.04683	0.300	2.03	0.02279
0.650	3.88	0.04269	0.200	1.62	0.01904

Results

Most of the thermophysical properties of the CHF_3 at 323.15 K and the pressure range used in this work have been reported in the literature. The critical parameters of the CHF_3 are T_c = 299.3 K, $p_c = 4.858$ MPa, and a critical density of $\rho_c = 0.529$ g/cm^3. The density of CHF_3 at 323.15 K, as a function of pressure, was taken from the data by Rubio et al.,[26] and the viscosity was reported by Altunin et al.[27] The dielectric constant of CHF_3 was measured by Reuter et al.[28] above the critical temperature up to 468 K and 200 MPa, and by the authors[22] in the density range of 0.21−0.91 g/cm^3. Table 1 summarizes the values of the dielectric constant (ϵ) and viscosity (η) in the range of densities studied in this work.

The conductivity of pure supercritical CHF_3 at 323.15 K in the density range of 0.294−0.915 g/cm^3 was measured in a previous work,[22] and the results for the dependence of the specific conductance κ° on the fluid density ρ were expressed in the form of a polynomial:

$$\log \kappa^\circ = -20.7470 + 44.1610\rho - 81.4748\rho^2 + 90.7700\rho^3 - 40.0522\rho^4 \quad (1)$$

where κ° is given in units of S/cm and ρ is given in units of g/cm^3. This expression has been used to correct the conductivity of the solutions by the effect of the solvent conductivity.

Electrical Conductivity of $TBAPF_6$ and $Fe(Cp^*)_2PF_6$ in Supercritical CHF_3. The molar conductivity of $TBAPF_6$ in supercritical CHF_3 at 323.15 K was measured in the density range of 0.29−0.91 g/cm^3, and the results are summarized in Table 2. The concentration of the salt ranged from 2.095×10^{-6} mol dm^{-3} to 6.511×10^{-4} mol dm^{-3}. The results for the highest concentration have been reported previously,[22] and they have been included in Table 2 for completeness.

The accuracy of the results decreases as the salt concentration decreases, because the measured resistance increases concomitantly and the solvent conductivity makes a large contribution, particularly at high densities. At concentrations of $>10^{-5}$ mol dm^{-3}, the solvent correction is <3% at all the densities studied. At densities of <0.40 g/cm^3, the accuracy is limited by the performance of the AC bridge in high-resistivity media. Because

TABLE 2: Molar Conductivity of $TBAPF_6$ in CHF_3 at 323.15 K

density, ρ (g/cm^3)	conductivity, Λ (S cm^2 mol^{-1})	density, ρ (g/cm^3)	conductivity, Λ (S cm^2 mol^{-1})
$c = 2.095 \times 10^{-6}$ mol dm^{-3}		$c = 7.469 \times 10^{-5}$ mol dm^{-3}	
0.9043	178.9	0.8979	66.1_5
0.8534	137.7	0.8536	47.5_9
0.8053	103.3	0.8040	32.0_0
0.7557	72.8_6	0.7551	20.8_8
0.7099	49.7_1	0.7107	13.7_4
0.6647	32.1_2	0.6650	8.69
0.6127	18.0_1	0.6122	4.85
0.5694	10.2_0	0.5673	2.80
0.5179	4.68	0.5173	1.42
0.4623	1.65	0.4629	0.538
0.4173	0.586		
0.3517	0.0856		
0.2965	0.0096		
$c = 8.499 \times 10^{-6}$ mol dm^{-3}		$c = 1.097 \times 10^{-4}$ mol dm^{-3}	
0.9022	160.4	0.9039	59.1_3
0.8527	116.6	0.8515	40.1_0
0.8041	81.8_9	0.8057	27.7_0
0.7552	55.1_2	0.7566	18.1_5
0.7120	37.4_6	0.7088	11.6_3
0.6650	23.6_0	0.6628	7.34
0.6086	12.70	0.6122	4.23
0.5688	7.68	0.5678	2.50
0.5161	3.59	0.5161	1.25
0.4588	1.31		
0.4167	0.539		
0.3499	0.0791		
$c = 1.932 \times 10^{-5}$ mol dm^{-3}		$c = 3.037 \times 10^{-4}$ mol dm^{-3}	
0.8938	111.1	0.8984	36.6_2
0.8541	84.0_7	0.8524	25.8_6
0.8046	57.3_6	0.8055	17.6_8
0.7548	37.6_8	0.7555	11.4_8
0.7103	24.9_7	0.7078	7.42
0.6654	15.8_9	0.6652	4.91
0.6109	8.76	0.6138	2.90
0.5678	5.03	0.5688	1.75
0.5156	2.39		
0.4588	0.885		
0.4162	0.362		
$c = 4.085 \times 10^{-5}$ mol dm^{-3}		$c = 6.511 \times 10^{-4}$ mol dm^{-3}[a]	
0.9028	87.4_0	0.9086	27.0_9
0.8520	60.6_1	0.8518	19.2_9
0.8041	41.5_0	0.8068	13.5_1
0.7541	26.9_4	0.7566	8.92
0.7111	18.0_0	0.7088	5.90
0.6647	11.2_7	0.6660	4.01
0.6164	6.33	0.6118	2.40
0.5688	3.68		
0.5167	1.77		
0.4582	0.638		
0.4162	0.224		

[a] Reported in ref 22.

of the solubility restrictions, the conductivity of solutions at concentrations of $>10^{-4}$ mol dm^{-3} could not be measured at densities of <0.50 g/cm^3.

In Table 3, we report the molar conductivity of $Fe(Cp^*)_2PF_6$ in supercritical CHF_3 at 323.15 K in the density range of 0.46−0.91 g/cm^3 and concentrations up to 4.88×10^{-3} mol dm^{-3}. The lower solubility[22] of this salt in supercritical CHF_3 limits the measurements to concentrations of $<10^{-5}$ mol dm^{-3} at densities of <0.60 g/cm^3.

The accuracy of the conductivity measurements decreases as the density increases, because of the high resistance of the solutions. Table 4 shows the mean values of several measurements of the molar conductivity and their corresponding standard deviation for saturated solutions in the low-density region. Note that errors in the molar conductivity are >2% at densities of <0.50 g/cm^3. However, experimental uncertainties are well below 1% for solutions at higher densities, which allows the treatment of the electrical conductivity data to obtain thermodynamic information, as we will describe later.

The molar conductivity (Λ), at densities of >0.45 g/cm^3, can be accurately fitted using a polynomial expression of the form

$$\Lambda = \sum_{i=1}^{4} a_i \rho^i \qquad (2)$$

Thus, we have calculated the values of the molar conductivity for both salts at selected interpolated densities; these values are reported in Table 5. The smoothed values of the molar conductivities of $TBAPF_6$ and $Fe(Cp^*)_2PF_6$, as a function of the square root of concentration at several densities in the range of 0.65−0.90 g/cm^3, are shown as solid lines in Figures 1 and

TABLE 3: Molar Conductivity of $Fe(Cp^*)_2PF_6$ in CHF_3 at 323.15 K

density, ρ (g/cm^3)	conductivity, Λ (S cm^2 mol^{-1})	density, ρ (g/cm^3)	conductivity, Λ (S cm^2 mol^{-1})
$c = 3.141 \times 10^{-6}$ mol dm^{-3}		$c = 6.135 \times 10^{-5}$ mol dm^{-3}[a]	
0.8051	287.3	0.9040	212.2
0.7543	230.5	0.8559	169.9
0.7072	173.1	0.8065	127.7
0.6633	123.6	0.7547	89.3
0.6122	76.8	0.7094	61.9
0.5678	47.1	0.6657	39.8
0.5144	22.5		
0.4588	7.56		
$c = 6.235 \times 10^{-6}$ mol dm^{-3}		$c = 8.025 \times 10^{-5}$ mol dm^{-3}	
0.8546	336.5	0.9047	194.5
0.8037	274.7	0.8545	153.2
0.7561	211.8	0.8059	115.2
0.7099	154.4	0.7528	79.7
0.6650	107.0	0.6951	49.8
0.6059	60.4		
0.5642	37.3		
0.5167	19.1		
$c = 9.994 \times 10^{-6}$ mol dm^{-3}		$c = 1.023 \times 10^{-4}$ mol dm^{-3}	
0.9058	367.3	0.9065	180.5
0.8515	311.1	0.8528	138.3
0.8034	250.3	0.8047	102.8
0.7527	185.2	0.7555	72.0
0.7083	134.4	0.6925	41.6
0.6583	87.8		
0.6065	52.2		
0.5495	26.2		
$c = 1.508 \times 10^{-5}$ mol dm^{-3}		$c = 1.431 \times 10^{-4}$ mol dm^{-3}	
0.9030	313.5	0.9056	160.9
0.8538	265.1	0.8560	124.9
0.8062	211.4	0.8039	90.5
0.7570	156.3	0.7533	62.4
0.7094	110.1		
0.6680	77.4		
0.6118	44.5		
0.5683	26.6		
$c = 1.985 \times 10^{-5}$ mol dm^{-3}		$c = 1.994 \times 10^{-4}$ mol dm^{-3}	
0.8518	244.7	0.9067	143.6
0.8047	193.7	0.8518	107.6
0.7586	145.8	0.7978	76.1
0.7102	102.3	0.7462	51.9
0.6626	68.6		
0.5946	34.5		
$c = 2.451 \times 10^{-5}$ mol dm^{-3}		$c = 3.057 \times 10^{-4}$ mol dm^{-3}	
0.9063	288.4	0.9062	121.6
0.8547	236.1	0.8521	90.3
0.8044	182.0	0.7970	63.2
0.7553	132.6		
0.7086	93.1		
0.6598	60.8		
0.5946	30.3		
$c = 3.130 \times 10^{-5}$ mol dm^{-3}		$c = 4.297 \times 10^{-4}$ mol dm^{-3}	
0.9050	264.0	0.9040	108.3
0.8519	212.1	0.8546	81.8
0.8041	164.0	0.8065	59.8
0.7600	123.1		
0.7119	85.5		
0.6633	55.6		
0.6109	30.6		
$c = 4.516 \times 10^{-5}$ mol dm^{-3}		$c = 4.882 \times 10^{-4}$ mol dm^{-3}	
0.9062	236.2	0.9061	103.2
0.8519	186.1	0.8522	76.6
0.8057	143.9	0.7982	52.4
0.7588	105.3		
0.7131	74.1		
0.6439	39.9		

[a] Reported in ref 22.

2, respectively. These figures also show the estimated values of the conductivities calculated with the parameters fitted with the Fuoss−Kraus conductivity equations with and without triple ions, as discussed below.

The general aspects of these curves are typical of highly associated electrolytes; that is, the molar conductivity decreases more rapidly than predicted by the Onsager limiting law, as shown in Figure 1 for $TBAPF_6$ at densities of 0.75−0.90 g/cm^3.

TABLE 4: Molar Conductivity of Saturated Solutions of $TBAPF_6$ and $Fe(Cp^*)_2PF_6$ in CHF_3 at 323.15 K

density, ρ (g cm^{-3})	concentration, c (mol dm^{-3})	conductivity, Λ (S cm^2 mol^{-1})
	$TBAPF_6$	
0.2946	$(6.81 \pm 0.04) \times 10^{-6}$	0.0088 ± 0.0005
0.3512	$(1.58 \pm 0.03) \times 10^{-6}$	0.0546 ± 0.0020
0.4156	$(4.10 \pm 0.04) \times 10^{-5}$	0.251 ± 0.012
0.4612	$(8.06 \pm 0.04) \times 10^{-5}$	0.549 ± 0.023
0.5185	$(1.88 \pm 0.04) \times 10^{-4}$	1.12 ± 0.03
0.5678	$(3.92 \pm 0.02) \times 10^{-4}$	1.75 ± 0.04
	$Fe(Cp^*)_2PF_6$	
0.2926	$(3.80 \pm 0.06) \times 10^{-7}$	0.042 ± 0.014
0.3502	$(9.06 \pm 0.06) \times 10^{-7}$	0.89 ± 0.24
0.4167	$(2.48 \pm 0.06) \times 10^{-6}$	3.63 ± 0.17
0.4591	$(4.70 \pm 0.03) \times 10^{-6}$	7.04 ± 0.25
0.5150	$(1.09 \pm 0.01) \times 10^{-5}$	13.1 ± 0.2
0.5659	$(2.36 \pm 0.01) \times 10^{-5}$	19.1 ± 0.2
0.6125	$(4.76 \pm 0.01) \times 10^{-5}$	23.5 ± 0.3

By comparing the molar conductivity of both salts at the same density as those reported in Table 5, it is clear that the molar conductivity of $Fe(Cp^*)_2PF_6$ is greater than that of $TBAPF_6$. This observation means that, in supercritical CHF_3 at a given density, the association constant of $TBAPF_6$ is higher than that of $Fe(Cp^*)_2PF_6$.

Association Constants and Infinite-Dilution Electrical Conductivity of $TBAPF_6$ and $Fe(Cp^*)_2PF_6$ in Supercritical CHF_3. The concentration dependence of the molar conductivity in electrolytes that exhibit ionic association can be described by the relation[29]

$$\Lambda = \Lambda^\circ - S\sqrt{\alpha c} + E\alpha c \ln(\alpha c) + J_1(d)\alpha c - J_2(d)(\alpha c)^{3/2} - K_A\Lambda\gamma_\pm^2\alpha c \quad (3)$$

where S is the limiting law slope, and E, J_1, and J_2 are parameters that are dependent on the closest distance of approach of the ions (d). The ion-pair formation constant (K_A) can be related to the degree of dissociation (α) by the relation

$$K_A = \frac{1-\alpha}{c\alpha^2\gamma_\pm^2} \quad (4)$$

Equation 3, along with the extended Debye−Hückel equation for the mean activity coefficient,

$$\ln \gamma_\pm = -\frac{A(\alpha c)^{1/2}}{1 - d\kappa} \quad (5)$$

are used to calculate Λ° and K_A from the conductivity data, by considering Λ°, K_A, and d to be adjustable parameters. Note that fitting the experimental conductivity data to eqs 3 and 5 requires very precise electrical conductivity measurements, such as those performed in normal solvents, where the ion association does not deplete the conductivity of the media.

When the ionic association is too strong, as in this case, eq 3 rarely converges and much simpler equations must be used to represent the electrical conductivity data. Fuoss and Kraus[30] derived an expression that allows the calculation of Λ° and K_A:

$$\frac{T(z)}{\Lambda} = \frac{1}{\Lambda^\circ} + \left(\frac{c\gamma_\pm^2\Lambda}{T(z)}\right)\left[\frac{K_A}{(\Lambda^\circ)^2}\right] \quad (6)$$

where $T(z) = 1 - z[1 - z(1 - ...)^{-1/2}]^{-1/2} \approx (1 - z)$, where $z = S(\Lambda c)^{1/2}/(\Lambda^\circ)^{3/2}$.

When the conductivity measurements are extended down to very diluted solutions, as in this case, a plot of $T(z)/\Lambda$ as a function of $c\gamma_\pm^2\Lambda/T(z)$ yields the values of $K_A/(\Lambda^\circ)^2$ and $1/\Lambda^\circ$ from the slope and the intercept, respectively. This relationship, which is often used to obtain initial values for Λ° and K_A to fit

TABLE 5: Molar Conductivity of $TBAPF_6$ and $Fe(Cp^*)_2PF_6$ in CHF_3 at 323.15 K, as a Function of Concentration at Several Densities (ρ)[a]

concentration, c (mol dm^{-3})	Molar Conductivity, Λ (S cm^2 mol^{-1})								
	$\rho = 0.90$	$\rho = 0.85$	$\rho = 0.80$	$\rho = 0.75$	$\rho = 0.70$	$\rho = 0.65$	$\rho = 0.60$	$\rho = 0.55$	$\rho = 0.50$
					$TBAPF_6$				
2.095×10^{-6}	175.2	135.2	99.7	69.6	45.6	27.7	15.3	7.70	3.59
8.499×10^{-6}	158.4	114.3	79.4	52.9	33.5	20.0	11.26	6.03	3.01
1.932×10^{-5}	116.0	81.4	55.4	35.2	22.6	13.45	7.56	4.02	1.94
4.065×10^{-5}	85.8	59.7	40.2	26.0	16.1	9.51	5.32	2.82	1.39
7.469×10^{-5}	67.2	46.3	30.9	20.0	12.4	7.37	4.19	2.25	1.09
1.097×10^{-4}	57.5	39.6	26.4	17.1	10.7	6.40	3.69	2.00	0.96
3.037×10^{-4}	37.1	25.4	16.9	10.93	6.89	4.22	2.50	1.37	
6.511×10^{-4}	25.8	18.9	12.9	8.33	5.37	3.55	1.92		
					$Fe(Cp^*)_2PF_6$				
3.141×10^{-6}	352.3	327.3	281.8	224.7	164.8	110.7	67.2	37.1	18.7
6.235×10^{-6}	376.4	331.5	269.8	204.0	143.4	93.3	56.4	31.4	
9.994×10^{-6}	362.4	309.4	245.7	182.0	125.8	81.1	48.7	26.4	
1.508×10^{-5}	310.9	261.0	204.1	149.2	102.0	65.4	39.2		
1.985×10^{-5}	291.6	242.8	188.7	137.5	94.3	61.1	36.8		
2.451×10^{-5}	282.5	231.1	177.2	127.8	86.7	55.4	32.4		
3.130×10^{-5}	259.4	210.1	160.0	114.6	77.4	48.7			
4.156×10^{-5}	230.7	184.3	138.9	98.8	66.5	42.3			
6.135×10^{-5}	208.8	164.6	122.5	86.2	56.9				
8.025×10^{-5}	190.7	149.6	110.9	78.1	52.4				
1.023×10^{-4}	175.3	136.1	99.8	68.8	44.5				
1.481×10^{-4}	156.7	120.4	88.4	60.6					
1.984×10^{-4}	138.9	106.1	77.7	53.4					
3.057×10^{-4}	117.8	89.2	64.5						
4.297×10^{-4}	106.0	79.5	57.1						
4.882×10^{-4}	100.1	75.6	53.2						

[a] Density values given in units of g/cm^3.

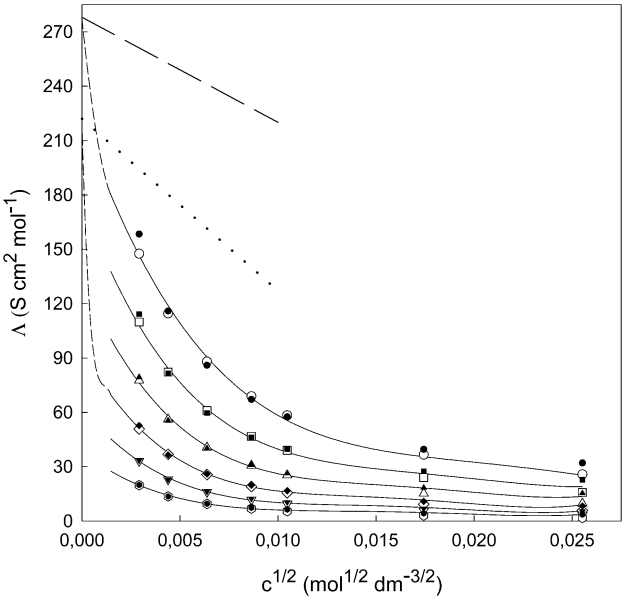

Figure 1. Molar conductivity of $TBAPF_6$ in CHF_3 at 323.15 K, as a function of concentration c at densities (from top to bottom) of ρ = 0.90, 0.85, 0.80, 0.75, 0.70, and 0.65 g/cm^3. Solid lines correspond to the smoothed experimental data (using eq 2). Open symbols correspond to the molar conductivities calculated with the Fuoss−Kraus parameters without triple ions (eq 6), and filled symbols correspond to those with triple ions (eq 7). The dashed and dotted lines are the corresponding Onsager slopes calculated from the data in Table 1 for ρ = 0.90 and 0.75 g/cm^3, respectively, starting at the corresponding limiting molar conductivities taken from the Fuoss−Kraus fit without triple ions. Dashed lines in the dilute region are present only as a guide to the eye.

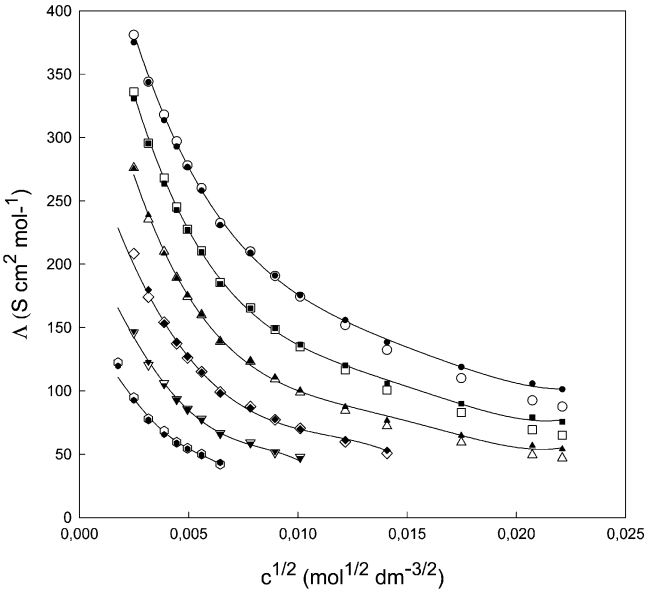

Figure 2. Molar conductivity of $Fe(Cp^*)_2PF_6$ in CHF_3 at 323.15 K, as a function of concentration c at densities (from top to bottom) of ρ = 0.90, 0.85, 0.80, 0.75, 0.70, and 0.65 g/cm^3. Solid lines correspond to the smoothed experimental data (using eq 2). Open symbols correspond to the molar conductivities calculated with the Fuoss−Kraus parameters without triple ions (eq 6), and filled symbols correspond to those with triple ions (eq 7).

eq 3, was used in this work to obtain the ion-pair formation constants and molar conductivities at infinite dilution for both salts. The results of fitting our conductivity data for $Fe(Cp^*)_2PF_6$ and $TBAPF_6$ to eq 6 are shown in Figures 3 and 4, respectively.

The estimated molar conductivities of both salts (using the fitted parameters $\Lambda°$ and K_A), along with the activity coefficients

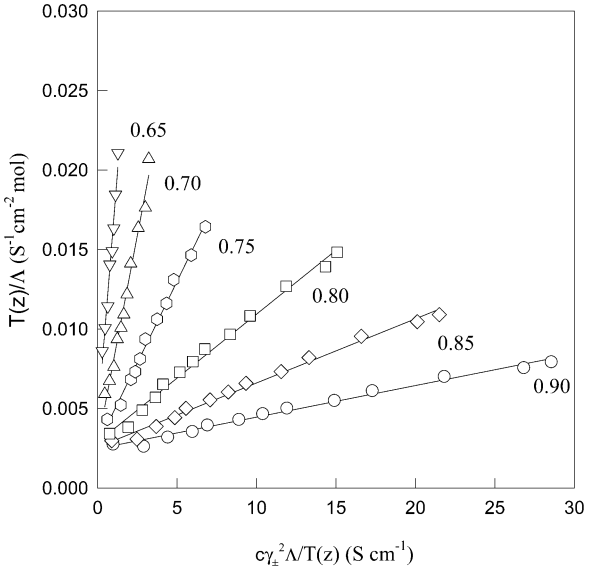

Figure 3. Fuoss−Kraus plots (without triplets) for $Fe(Cp^*)_2PF_6$ in CHF_3 at 323.15 K at several densities (densities, in units of g/cm^3, are indicated in the plots).

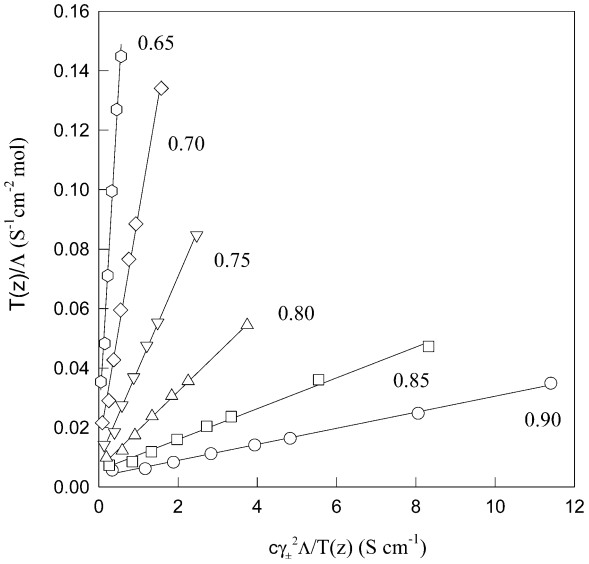

Figure 4. Fuoss−Kraus plots (without triplets) for $TBAPF_6$ in CHF_3 at 323.15 K at several densities (densities, in units of g/cm^3, are indicated in the plots).

obtained from eq 5 (using the Bjerrum distance of closest approach, $d_{Bj} = |z_i z_j| e^2/(2\epsilon kT)$, where z is the valency of the ion, e the electron charge, and k the Boltzmann constant), are shown in Figures 1 and 2. The fit was performed for salt concentrations of $>6 \times 10^{-6}$ mol dm^{-3}; that is, the more-diluted concentration for each density was not considered. The maximum concentration of the fit for $TBAPF_6$ was 6.5×10^{-4} mol dm^{-3} at densities of >0.8 g/cm^3 and 1×10^{-4} mol dm^{-3} at densities of <0.80 g/cm^3. For $Fe(Cp^*)_2PF_6$, the maximum concentration of the fit was 1×10^{-4} mol dm^{-3} at densities of >0.80 g/cm^3 and 5×10^{-5} mol dm^{-3} at densities of <0.80 g/cm^3.

The calculated values shown in Figures 1 and 2 extend to concentrations beyond the corresponding maximum, and, for this reason, the calculated molar conductivity deviates from the experimental values at high concentrations. If high-concentration values are considered in the fit of the Fuoss−Kraus equation without triple ions (eq 6), the standard deviation deteriorates in the dilute region, and it can be considered as an indication of the triple-ion formation in this concentration region.

TABLE 6: Molar Conductivity at Infinite Dilution and Association Constants for $Fe(Cp^*)_2PF_6$ in Supercritical CHF_3 at 323.15 K

		Molar Conductivity at Infinite Dilution, $\Lambda°$ (S cm^2 mol^{-1})					
			Experiment		K_A (10^{-5}dm^3 mol^{-1})		
density, ρ (g/cm^3)	d_{Bj} (10^{-8} cm)	Walden rule	with triplets (eq 7)	without triplets (eq 6)	with triplets (eq 7)	without triplets (eq 6)	K_T (10^{-2} dm^3 mol^{-1})
0.90	45.4	770	475 ± 5	493 ± 11	0.62 ± 0.02	0.62 ± 0.04	4.6 ± 0.3
0.85	49.06	823	475 ± 5	495 ± 16	1.2 ± 0.03	1.2 ± 0.1	3.8 ± 0.15
0.80	52.80	923	480 ± 10	478 ± 24	2.4 ± 0.1	2.3 ± 0.3	3.7 ± 0.3
0.75	56.95	989	500 ± 100	419 ± 33	5.8 ± 2.4	3.7 ± 0.7	4.0 ± 0.9
0.70	61.56	1106	400 ± 100	337 ± 34	8.7 ± 4.6	5.4 ± 1.3	7.0 ± 5.5
0.65	66.64	1186	300 ± 200	233 ± 33	14 ± 19	6.2 ± 2.1	42 ± 26

TABLE 7: Molar Conductivity at Infinite Dilution and Association Constants for $TBAPF_6$ in Supercritical CHF_3 at 323.15 K

		Molar Conductivity at Infinite Dilution, $\Lambda°$ (S cm^2 mol^{-1})					
			Experiment		K_A (10^{-5}dm^3 mol^{-1})		
density, ρ (g/cm^3)	d_{Bj} (10^{-8} cm)	Walden rule	with triplets (eq 7)	without triplets (eq 6)	with triplets (eq 7)	without triplets (eq 6)	K_T (10^{-2} dm^3 mol^{-1})
0.90	45.4	770	400 ± 10	278 ± 16	5.1 ± 0.3	1.9 ± 0.2	7.8 ± 0.35
0.85	49.06	823	390 ± 10	262 ± 28	10.9 ± 0.6	4.0 ± 1.0	9.6 ± 0.3
0.80	52.80	923	405 ± 10	247 ± 30	27.5 ± 1.5	8.7 ± 2.4	10.2 ± 0.4
0.75	56.95	989	325 ± 50	222 ± 142	41 ± 14	18 ± 25	4.9 ± 0.6
0.70	61.56	1106	300 ± 100	255 ± 97	92 ± 63	65 ± 52	6.2 ± 0.4
0.65	66.64	1186	350 ± 150	181 ± 65	371 ± 330	93 ± 69	9.9 ± 0.5

The reduced temperature, $T^* = kT\epsilon\sigma/(|z_+z_-|e^2)$, where ϵ is the dielectric constant of the solvent and σ is the sum of the crystallographic radii of the anion and the cation, is used as a parameter to determine the extent of ion clustering in ionic solutions.[31] If T^* is very low, the contribution of the charged triple ions to the conductivity become important. In that case, the Fuoss−Kraus equation becomes[30]

$$\Lambda g(c)c^{1/2} = \frac{\Lambda°}{K_A^{1/2}}\frac{\Lambda°_T K_T}{K_A^{1/2}}\left(1 - \frac{\Lambda}{\Lambda°}\right)c \qquad (7)$$

where

$$g(c) = \frac{\gamma_\pm}{(1 - z)(1 - \Lambda/\Lambda°)^{1/2}} \qquad (8)$$

K_T is the formation constant of triple ions and $\Lambda°_T$ is the molar conductivity at infinite dilution of the triple ions. Usually, K_A and K_T are obtained from eq 7, using an estimated value of $\Lambda°$ that has been calculated from Walden's rule ($\Lambda°\eta$ = constant) and assuming that $\Lambda°_T = 2\Lambda°/3$. This procedure was adopted by Abbott and Eardley[21] to fit the conductivity data of $TBABF_4$ in supercritical difluoromethane using the Fuoss−Kraus equation for triple ions.

However, the validity of Walden's rule has not been tested in these low-temperature supercritical fluids, and it is one of the goals of this work. For this reason, we have obtained the formation constants by fitting the value of $\Lambda°$ that minimizes the standard deviation of the linear fit of eq 7.

The results of the fitting of $\Lambda°$ and the formation constants are summarized in Tables 6 and 7, for $TBAPF_6$ and $Fe(Cp^*)_2PF_6$, respectively. In this case, the fit improves when the higher-concentration values are used. Thus, the minimum concentration for the fit was 8×10^{-6} mol dm^{-3} for $TBAPF_6$, whereas, for $Fe(Cp^*)_2PF_6$, the minimum concentration increases from 3×10^{-6} mol dm^{-3} at a density of 0.65 g/cm^3 up to 4×10^{-5} mol dm^{-3} at a density of 0.90 g/cm^3. The errors reported for K_A and K_T were obtained from the uncertainty in $\Lambda°$ and the corresponding statistical uncertainties of the intercept and slope of eq 7.

The molar conductivities calculated with the parameters of the Fuoss−Kraus equation with triple ions (eq 7) are shown in Figures 1 and 2. Except for $TBAPF_6$ at the higher densities, the Fuoss−Kraus fit with triplets is better than the fit without triplets in the more-concentrated region, whereas the difference between both fits are negligible in the dilute region of the concentration range studied here.

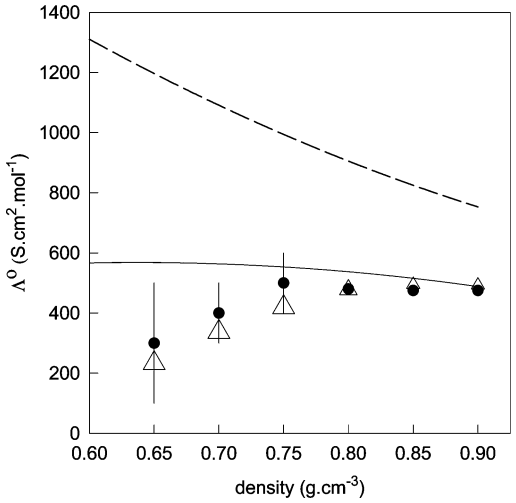

Figure 5. Molar conductivity at infinite dilution for $Fe(Cp^*)_2PF_6$ in CHF_3 at 323.15 K, as a function of density (Fuoss−Kraus equation results (●) with and (△) without triplets). Errors in $\Lambda°$, when larger than the symbol size, are indicated with vertical bars. Dashed line represents the estimation using Walden's rule, and the solid line denotes the results of the CC model.

The change of $\Lambda°$, relative to density ρ, for $Fe(Cp^*)_2PF_6$ is shown in Figure 5 for both versions of the Fuoss−Kraus equation. It is clear that the molar conductivity at infinite dilution for this electrolyte in supercritical CHF_3 remains constant at densities of >0.75 g/cm^3 and decrease as the density decreases below that density.

In a previous work,[32] we studied the conductivity of $Fe(Cp^*)_2PF_6$ and $TBAPF_6$ in organic solvents of low dielectric constant. That work showed that the Walden product ($\Lambda°\eta$) of $Fe(Cp^*)_2PF_6$ decreases slightly as the dielectric constant increases over the range studied ($20.9 < \epsilon < 8.9$), mainly because of the contribution of the PF_6^- anion (the dielectric friction of the bulky $Fe(Cp^*)_2^+$ ion is small and the Walden product is expected, in this case, to be independent of the solvent polarity).

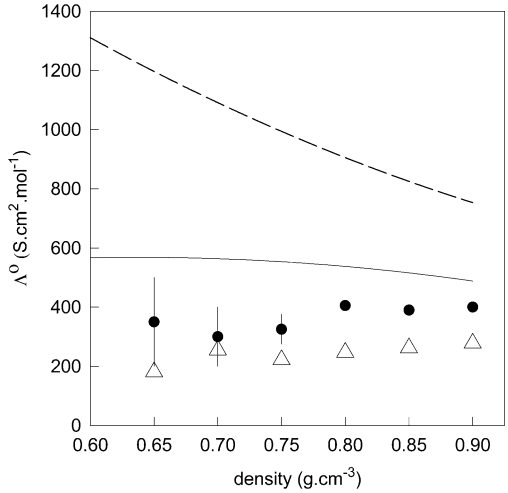

Figure 6. Molar conductivity at infinite dilution for $TBAPF_6$ in CHF_3 at 323.15 K, as a function of density (Fuoss−Kraus equation results (●) with and (△) without triplets). Errors in $\Lambda°$ are only plotted for the Fuoss−Kraus equation with triplets. Dashed line represents the estimation using Walden's rule, and the solid line denotes the results of the CC model.

If the dependence of electrical conductivity that is observed in subcritical incompressible liquids were used to predict the conductivity of $Fe(Cp^*)_2PF_6$ in supercritical CHF_3, a decrease in $\Lambda°$ with increasing densities should be expected, because of the increasing viscosity. This seems to be in clear contrast with our experimental results, as shown in Figure 5.

Figure 6 shows the same results for $TBAPF_6$ in supercritical CHF_3. In this case, the molar conductivity at infinite dilution is almost constant over the entire range of density and also exhibits the opposite behavior, as predicted by Walden's rule if we assume that it is valid in supercritical CHF_3.

The failure of Walden's rule to predict the dependence of the molar conductivity at infinite dilution, relative to density (that is, the unavailability of the classical hydrodynamic model to describe ionic mobility in supercritical fluids), is not unexpected. It was first evidenced by Marshall's conductivity studies in supercritical water[33] and later confirmed with higher-precision measurements by Wood and co-workers[7,8] and also predicted by computer simulation[34−36] and a semicontinuum model.[37] The compressible continuum solvent model (CC model)[38,39] was used by Xiao and Wood[40] to predict the conductivity of NaCl in supercritical water. They found that Walden's rule is not obeyed in this compressible media and that the CC model describes the limiting conductivity at densities of >0.5 g/cm^3 very well.

The CC model[38,39] accounts for the increase of density of the solvent in the vicinity of ions by the electric field ($E = ze/(4\epsilon_0\epsilon r^2)$). Assuming that the solvent compressibility (κ_T) is independent of the electric field, the relation between E and ρ is

$$E^2 = \int_p^0 \left[\frac{2}{\epsilon_0 \rho^2 \kappa_T (\partial\epsilon/\partial\rho)_{E,T}}\right] d\rho \qquad (9)$$

where ϵ_0 is the permittivity of a vacuum. The density $\rho(r)$ and the isothermal compressibility of supercritical CHF_3 at 323 K were derived from the available data[26] (reported as the Strobridge equation of state, $p(\rho,T)$) at pressures up to 103 MPa. The density derivative of the relative dielectric permittivity for CHF_3 was calculated using the $\epsilon(\rho)$ equation that has been previously reported.[22] The radius-dependent density yields a distance-dependent viscosity $\eta(r)$, which is calculated from the dependence, relative to density, of the viscosity of CHF_3 up to 40 MPa, which is obtained from the literature.[27,41]

The simplest version of the CC model, which only accounts for the electrostriction effect, was used, because no data for the Debye relaxation times for CHF_3 are available to calculate the electroviscous effect.[40]

Finally, the limiting conductivity for this CC model is finally calculated by the following expression:[42]

$$\Lambda° = Fe\int_\infty^R \frac{dr}{4\pi r^2 \eta(r)} \qquad (10)$$

where F is the Faraday constant and r is the distance from a spherical ion of radius R.

The choice of R for each ion determines the absolute values of the limiting ionic conductivities. Xiao and Wood[40] used the crystallographic radius for Na^+ and Cl^- ions; however, they adjusted the hydrodynamic radius of the water molecule in the electroviscous effect on the viscosity. In this case, for the radius of the ions, we adopted those obtained previously in the study of the electrical conductivity in low-permittivity solvents:[32] that is, 0.585 nm for the PF_6^- ion, and 0.409 nm for the TBA^+ and $Fe(Cp^*)_2^+$ ions. The results obtained for $\Lambda°$ are plotted in Figures 5 and 6, showing that the CC model predicts a completely different behavior for $\Lambda°$ than the continuum incompressible model (Walden's rule).

Discussion

The trends observed for the change of the molar conductivity at infinite dilution, relative to density, in CHF_3 is similar to that already observed experimentally for single electrolytes[5−8,43] in supercritical water. The present study constitutes the first experimental confirmation of the failure of the uncompressible continuum model in low-temperature supercritical fluids, such as fluoromethanes.

The weak density dependence of the molar conductivity at infinite dilution, observed for both salts in this variable-density supercritical medium, suggests that the change of the bulk fluid viscosity alone is insufficient to justify such trends. The reduction in the dielectric constant of CHF_3, which is associated to a decrease in density, might indicate that a dielectric friction contribution should be added to the viscous friction, to account for the observed behavior. However, the Walden product for $Fe(Cp^*)_2PF_6$ and $TBAPF_6$ in supercritical CHF_3 verifies a much stronger dependence on the dielectric constant than that observed for those same salts in liquid organic solvents,[32] which indicates that additional effects that are not necessarily related to solvent dipole relaxation should be invoked to explain the present experimental results.

The CC model predicts a very small increase in $\Lambda°$ when the density decreases from 0.9 g/cm^3 to 0.6 g/cm^3, in contrast with the larger density dependence that was observed by Xiao and Wood[40] in supercritical water.

Figure 5 shows that the limiting electrical conductivity for $Fe(Cp^*)_2PF_6$ calculated with the CC model, with the ionic radius obtained from electrical conductivity measurements in subcritical solvents, agrees quite well with the experimental data at the higher densities. At densities of <0.7 g/cm^3, the CC model overestimates $\Lambda°$. The disagreement could be due to an increase of the solvation radius of the $Fe(Cp^*)_2^+$ ion as the density approaches the critical density of the solvent.

Figure 6 shows that the CC model predicts a larger conductivity for $TBAPF_6$ when the radius in subcritical solvents are

used. Indeed, the agreement at high densities is quite good if the radius of the TBA^+ cation is fixed at ~0.55 nm. On the other hand, the CC model seems to describe the almost-independence of $\Lambda°$, relative to density, correctly. Thus, one could speculate that the solvation radius of the TBA^+ ion does not change in the low-density region or it changes at densities of <0.6 g/cm^3.

The results in supercritical CHF_3 reinforce the view already accepted for supercritical water: in the low-density supercritical region, the reduction of the ion mobility is related to the increase of the local solvent density around ions. More precisely, one could assume a more-rigid ionic solvation shell (the *solvent−berg* model) in the low-density region, and, thus, an increasing friction on the ion.

In fact, the tendency of supercritical solvents to increase their local density around solutes is dependent on the attractive solvent−solute potential and the solvent compressibility, which occurs at densities below the critical density.[44] The isothermal compressibility of CHF_3 at the temperature used in this work ($T/T_c = 1.08$) is almost a factor 2 greater than that of water at the same reduced temperature, which indicates that any local density effect in the supercritical region could be enhanced for CHF_3, in relation to water. We also recognize that interactions between water and ions may be expected to be stronger than those between CHF_3 and ions, because of a higher dipolar moment. However, the CC model results for $\Lambda°$ seem to indicate that the higher compressibility of CHF_3, in comparison to that of supercritical water, is responsible for the lower increase of $\Lambda°$ with decreasing density.

The extremely low solubility of small ions in CHF_3 makes a direct comparison with water impossible. However, it is plausible that the behavior of the limiting molar conductivity observed in water and CHF_3 is common to all supercritical fluids: the density region where the *solvent−berg* behavior predominates is dependent on the particular ion−solvent interactions.

The ion-pair formation constant for $Fe(Cp^*)_2PF_6$ and $TBAPF_6$ increases as T^*—and, consequently, ρ—decrease, as predicted by common models of ion association.[29] The results in Tables 6 and 7 show that the K_A value for $Fe(Cp^*)_2PF_6$ is less than that for $TBAPF_6$ over the entire density range, even when the crystallographic radius of $Fe(Cp^*)_2PF_6$ is smaller. Figure 7 shows the ion-pair formation constant of both electrolytes, plotted as a function of $(\epsilon T)^{-1}$, including supercritical CHF_3 results and also those obtained in organic solvents.[32] It is observed that the behavior described previously is also present in subcritical solvents and that the reduction of the density enhances the difference in ion-pair formation. A possible explanation for this behavior could be the tendency of $Fe(Cp^*)_2PF_6$ to form solvent-separated ion pairs, which would increase in the low-density region. The decrease of $\Lambda°$ with decreasing density supports this claim.

Note that the effect of local inhomogeneities in supercritical HFCs and water impact the observed behavior of the limiting molar conductivity with decreasing density, instead of the ion-cluster formation constants. It has been remarked[45] that different experiments probe the local and long-range density inhomogeneities in supercritical fluids. Our results show that the limiting conductivity is more sensitive than the ion-pair formation constant to local density effects. This is expected, on the basis that the ion pairing is mainly a function of the dielectric constant, which decreases steadily as the density increases, whereas the limiting ionic conductivity has two opposite contributions when density decreases: a reduction of the friction, which is due to the depletion of the bulk viscosity, and an increase in friction, which is due to the rigid solvation shell around the ions. The last effect prevails in the low-density region.

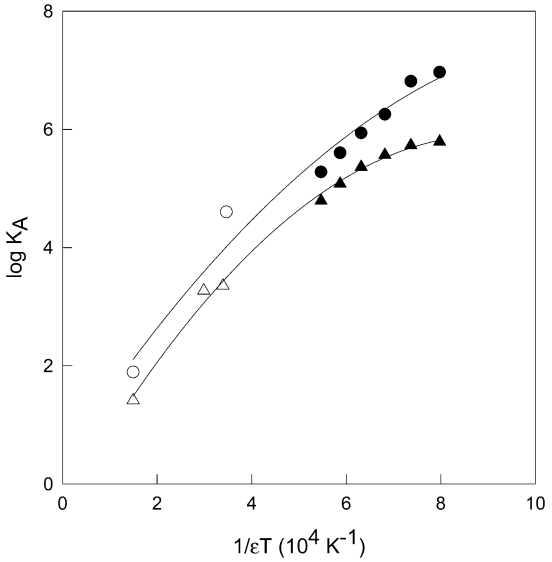

Figure 7. Ion-pair formation constants, as a function of the solvent polarity: (●) $TBAPF_6$ in supercritical CHF_3 at 323.15 K, (▲) $Fe(Cp^*)_2PF_6$ in supercritical CHF_3 at 323.15 K, (○) $TBAPF_6$ in acetone and dichloromethane at 298.15 K,[31] and (△) $Fe(Cp^*)_2PF_6$ in acetone, dichloroethane, and dichloromethane at 298.15 K.[31]

Conclusions

The electrical conductivity of tetrabutylammonium hexafluorophosphate ($TBAPF_6$) and decamethylferrocenium hexafluorophosphate ($Fe(Cp^*)_2PF_6$) in supercritical trifluoromethane (CHF_3) was measured at a temperature of 323.15 K, as a function of density. The concentration dependence of the molar conductivity ($\Lambda°$) was used to calculate the electrical conductivity at infinite dilution and the ion-pair formation constant of both electrolytes, as a function of the solvent density. The electrical conductivity at infinite dilution remained constant at densities of >0.75 g/cm^3 and decreased as the density decreased below that density for both electrolytes; the effect was more pronounced in the case of $Fe(Cp^*)_2PF_6$.

The compressible continuum solvent (CC) model qualitatively describes some of this behavior by allowing the ion−solvent friction increase at low density, which is due to the local viscosity increment by electrostriction. The decrease of $\Lambda°$ observed in the low-density region requires an explanation in terms of a *solvent−berg* view of the low-density region of the supercritical solvent, which is also observed in supercritical water, where the ion−solvent interaction, coupled to a high solvent compressibility, enhances the formation of a rigid solvation shell around the ions. This is equivalent to an increase in the solvation radius R of the ion in eq 10.

Ion association increases as the density decreases (or the dielectric constant decreases) for both ions; the ion-pair formation is more important for $TBAPF_6$ than for $Fe(Cp^*)_2PF_6$, probably because of the presence of solvent-separated ion pairs for the last salt.

Contrary to the conclusions reported from the analysis of the conductivity of tetrabutylammonium tetrafluoroborate ($TBABF_4$) in supercritical difluoromethane,[21] our analysis of the Walden product indicates that this simple incompressible continuum model is not valid in supercritical CHF_3. This is consistent with the presence of large local solvent density fluctuations around

the ions, mainly in the low-density region, which increases the ion friction, as compared to normal solvents.

The similarities observed in the results obtained for these electrolytes in supercritical CHF_3 and those previously reported for simple electrolytes in supercritical water help to understand the common nature of transport properties and speciation in supercritical fluids.

Acknowledgment. Work performed as part of CNEA-CAC-UAQ Project P5-36-3. Financial support from CONICET (PID 384/98) is greatly appreciated. H.R.C. is a member of Carrera del Investigador Científico del Consejo Nacional de Investigaciones Científicas y Técnicas (CONICET). D.L.G. thanks CNEA for a graduate fellowship.

References and Notes

(1) Fogo, J. K.; Benson, S. W.; Copeland, C. S. *J. Chem. Phys.* **1954**, *22*, 212.
(2) Franck, E. U. *Z. Phys. Chem.* **1956**, *8*, 92, 107, 192.
(3) Quist, S.; Marshall, W. L. *J. Phys. Chem.* **1966**, *70*, 3714; **1968**, *72*, 684, 1545, 2100, 3122; **1969**, *73*, 978.
(4) Ho, P. C.; Palmer, D. A.; Mesmer, R. E. *J. Solution Chem.* **1994**, *23*, 907.
(5) Ho, P. C.; Palmer, D. A. *J. Solution Chem.* **1996**, *25*, 711.
(6) Ho, P. C.; Palmer, D. A. *Geochim. Cosmochim. Acta* **1997**, *61*, 3027.
(7) Zimmerman, G. H.; Gruszkiewicz, M. S.; Wood, R. H. *J. Phys. Chem.* **1995**, *99*, 11612.
(8) Gruszkiewicz, M. S.; Wood, R. H. *J. Phys. Chem. B* **1997**, *101*, 6549.
(9) Flarsheim, W. M.; Tsou, Y.; Tratchtenberg, I.; Johnston, K. P.; Bard, A. J. *J. Phys. Chem.* **1986**, *90*, 3857.
(10) Liu, C.; Snyder, S. R.; Bard, A. J. *J. Phys. Chem. B* **1997**, *101*, 1180.
(11) Crooks, R. M.; Fan, F.-R. F.; Bard, A. J. *J. Am. Chem. Soc.* **1984**, *106*, 6851.
(12) Crooks, R. M.; Bard, A. J. *J. Phys. Chem.* **1987**, *91*, 1274.
(13) Cabrera, C. R.; García, E.; Bard, A. J. *J. Electroanal. Chem.* **1989**, *260*, 457.
(14) Crooks, R. M.; Bard, A. J. *J. Electroanal. Chem.* **1988**, *243*, 117.
(15) Cabrera, C. R.; Bard, A. J. *J. Electroanal. Chem.* **1989**, *273*, 147.
(16) Niehaus, D.; Philips, M.; Michael, A.; Wightman, R. M. *J. Phys. Chem.* **1989**, *93*, 6232.
(17) Abbott, A. P.; Harper, J. C. *J. Chem. Soc., Faraday Trans.* **1996**, *92*, 3895.
(18) Olsen, S. A.; Tallman, D. E. *Anal. Chem.* **1994**, *66*, 503.
(19) Olsen, S. A.; Tallman, D. E. *Anal. Chem.* **1996**, *68*, 2054.
(20) Abbott, A. P.; Eardley, C. A.; Harper, J. C.; Hop, E. G. *J. Electroanal. Chem.* **1998**, *457*, 1.
(21) Abbott, A. P.; Eardley, C. A. *J. Phys. Chem. B* **2000**, *104*, 9351.
(22) Goldfarb, D. L.; Corti, H. R. *Electrochem. Commun.* **2000**, *2*, 663.
(23) Goldfarb, D. L.; Corti, H. R. *J. Phys. Chem. B* **2004**, *108*, 3368−3375.
(24) Duggan, D. M.; Hendrickson, D. N. *Inorg. Chem.* **1975**, *14*, 955.
(25) Fernández, D. P.; Goodwin, A. R. H.; Levelt Sengers, J. M. H. *Int. J. Thermophys.* **1995**, *16*, 929.
(26) Rubio, R. G.; Zollweg, J. A.; Street, W. B. *Ber. Bunsen−Ges.* **1989**, *93*, 791.
(27) Altunin, V. V.; Geller, V. Z.; Petrov, E. K.; Rsskazov, D. C.; Spiridinov, G. A. *Thermophysical Properties of Freons*; Selover, T. B., Jr., Ed.; Methane Series, Part 1; Hemisphere Publishing Co.: Washington, DC, 1987.
(28) Reuter, K.; Rosenzweig, S.; Franck, E. U. *Physica A* **1989**, *156*, 294.
(29) Fernández-Prini, R. *Physical Chemistry of Organic Solvent Systems.* Covington, A. K., Dickinson, T., Eds.; Plenum Press: New York, 1973; Chapter 5.
(30) Fuoss, R. M.; Kraus, C. A. *J. Am. Chem. Soc.* **1933**, *55*, 2387.
(31) Corti, H. R.; Fernández-Prini, R. *J. Chem. Soc., Faraday Trans.* **1986**, *82*, 921.
(32) Goldfarb, D. L.; Longinotti, M. P.; Corti, H. R. *J. Solution Chem.* **2001**, *30*, 307.
(33) Marshall, W. L. *J. Chem. Phys.* **1987**, *87*, 3639.
(34) Lee, S. H.; Cummings, P. T.; Simonson, J. M.; Mesmer, R. E. *Chem. Phys. Lett.* **1998**, *293*, 289.
(35) Lee, S. H.; Cummings, P. T. *J. Chem. Phys.* **2000**, *112*, 864.
(36) Hyun, J.-K.; Johnston, K. P.; Rossky, P. J. *J. Phys. Chem. B* **2001**, *105*, 9302.
(37) Balbuena, P. B.; Johnston, K. P.; Rossky, P. J.; Hyun, J.-K. *J. Phys. Chem. B* **1998**, *102*, 3806.
(38) Wood, R. H.; Quint, J. R.; Grolier, J.-P. E. *J. Phys. Chem.* **1981**, *85*, 3944.
(39) Quint, J. R.; Wood, R. H. *J. Phys. Chem.* **1985**, *89*, 380.
(40) Xiao, C.; Wood, R. H. *J. Phys. Chem. B* **2000**, *104*, 918.
(41) Raskazov, D. S.; Babikov, U. M.; Filatov, N. Y. *Tr. Mosk. Energ. Inst.* **1975**, *234*, 90.
(42) Wolynes, P. G. *Annu. Rev. Phys. Chem.* **1980**, *31*, 345.
(43) Ibuki, K.; Ueno, M.; Nakahara, M. *J. Phys. Chem. B* **2000**, *104*, 5139.
(44) Fernández-Prini, R.; Japas, M. L. *Chem. Soc. Rev.* **1994**, *23*, 155.
(45) Tucker, S. C. *Chem. Rev.* **1999**, *99*, 391.